Universality and the three-body parameter of ^{4}He trimers

Pascal Naidon,[1] Emiko Hiyama,[1] and Masahito Ueda[2]
[1]*RIKEN Nishina Centre, RIKEN, Wako 351-0198, Japan*
[2]*Department of Physics, University of Tokyo, 7-3-1 Hongo, Bunkyo-ku, Tokyo 113-0033, Japan*
(Received 27 September 2011; revised manuscript received 24 May 2012; published 9 July 2012)

We consider a system of three ^{4}He atoms, which is so far the simplest realistic three-body system exhibiting the Efimov effect, in order to analyze deviations from the universal Efimov three-body spectrum. We first calculate the bound states using a realistic two-body potential, and then analyze how they can be reproduced by simple effective models beyond Efimov's universal theory. We find that the nonuniversal variations of the ground and first excited states can be well reproduced by models parametrized with only three quantities: the scattering length and effective range of the original potential, and a small three-body force. Furthermore, the three-body parameter, which fixes the origin of the infinite set of three-body levels, is found to be consistent with recent experimental observations in other atomic species.

DOI: 10.1103/PhysRevA.86.012502 PACS number(s): 31.15.ac, 67.85.−d, 03.65.Ge, 36.40.−c

I. INTRODUCTION

The universal attraction found by Efimov [1] for any quantum system of three particles interacting through short-range interactions with a large scattering length has now been evidenced in many experiments using ultracold atoms [2–17]. In particular, Efimov trimers, i.e., three-body bound states resulting from this attraction, were observed as a function of the scattering length. Because these trimers are unusually large compared with the range of the interactions, they have universal properties determined solely by the universal attraction and a few parameters. In particular, their spectrum has a simple structure with discrete scale invariance. This was confirmed experimentally to some degree, but there appeared quantitative deviations from this universal structure.

One of the main reasons is the fact that at most the ground and first-excited states of the spectrum could be observed so far. It is known that these first states do not follow accurately the universal behavior expected for the higher excited states (more loosely bound states) because their size is not very large compared to the range of the interactions and therefore they still depend on the details of these interactions. However, it is quite involved to correctly describe these interactions for three atoms because of their complex hyperfine structure and the lack of knowledge of the three-body potential surfaces. For this reason, experimental results have been interpreted so far using either corrections to the universal theory of Efimov [15,16,18,19] or by other effective models reproducing the two-body physics in the energy range of the observed trimers [20–22].

While these effective approaches can reproduce the experimental results to some extent, it remains unclear on a theoretical basis why they can do so. For example, corrections to the Efimov universal theory sometimes require one to introduce an *ad hoc* variation of a three-body parameter to explain the data [15,16,22]. Another puzzling fact is that effective two-body model approaches could reproduce some of the deviations from universal theory observed in the experimental data, suggesting that they could be explained by two-body interactions only [20–22]. While it is established that in general the knowledge of two-body interactions only is not enough to accurately determine the energy of Efimov trimers [23], the contribution from realistic two-body interactions to the short-range three-body phase and nonuniversal deviations is not fully understood.

The purpose of this paper is to clarify these issues by testing the effective approaches with respect to the numerically exact solution of a realistic theoretical model. We choose ^{4}He$_3$, as it is the simplest triatomic system with van der Waals interactions that exhibits the Efimov attraction [24–28].

The paper is organized as follows. In Sec. II, we review some of the effective models used to describe Efimov trimer experiments. In Sec. III, we present realistic calculations for ^{4}He$_3$, and show how they are reproduced by these effective models.

II. EFFECTIVE MODELS FOR EFIMOV PHYSICS

A. Efimov's universal theory

The essence of the Efimov effect is the appearance of an effective attractive potential $-s_0^2/R^2$ between three particles with very large scattering length. Here, s_0 is a number approximately equal to 1.00624 for identical bosonic particles and R denotes the hyper-radius (average distance between particles),

$$R^2 = \tfrac{1}{3}\left(r_{12}^2 + r_{23}^2 + r_{31}^2\right), \tag{1}$$

where r_{12}, r_{23}, and r_{31} are the relative distances between the three particles. This attraction can lead to the existence of three-body bound states, the so-called Efimov trimers. Because it is a long-range attraction, trimers with sufficiently small binding energy extend to large distances where the interactions are negligible. The effect of interactions is therefore captured by simply setting two types of short-distance boundary conditions on the three-body wave function. The first type of boundary condition is applied when two particles come close to one another, but within a distance r larger than the range of their interaction. There, the wave function ψ has to satisfy the Bethe-Peierls boundary condition,

$$\psi \underset{r_{ij}\to 0}{\propto} \frac{1}{r_{ij}} - \frac{1}{a}, \tag{2}$$

where a is the s-wave scattering length of the two-body interaction, which fixes the phase of the two-body wave

function accumulated at low energy within the range of the interaction. The second type of boundary condition is applied when three particles come close together, but still at distances R larger than the range of their interactions. The wave function has to satisfy the Efimov boundary condition,

$$\psi \underset{R\to 0}{\propto} \frac{1}{R}\sin[s_0 \ln(\Lambda R)], \tag{3}$$

where Λ is the so-called Efimov three-body parameter, which fixes the accumulated phase of the three-body wave function at low energy.

The Efimov theory thus relies on only two parameters, a and Λ, to fully describe the three-body physics in the low-energy and large-a regime. When normalized in units of Λ, the trimer energy spectrum exhibits a universal structure as a function of $a\Lambda$, as represented in Fig. 5. There is an accumulation point in the spectrum at $a=\infty$, which is when the two-body interaction is resonant, and the whole spectrum is invariant by a discrete scale transformation, namely, multiplying all distances by $e^{\pi/s_0}\approx 22.7$, which follows from Eq. (3). The wave functions and energies can be calculated numerically by either solving the three-body free Schrödinger equation with conditions (2) and (3), or equivalently solving its corresponding integral equation, which is known as the Skorniakov-Ter-Martirosian equation [29],

$$\left(\frac{1}{a}-\sqrt{\frac{3}{4}p^2-\varepsilon}\right)F(p) + \frac{2}{\pi}\int_0^P dq \ln\frac{p^2+q^2+pq-\varepsilon}{p^2+q^2-pq-\varepsilon}F(q)=0, \tag{4}$$

where F is the function to be determined (related to the full wave function Ψ), and $\varepsilon=\frac{mE}{\hbar^2}$ is the renormalized energy E, with m being the mass of the particle. Here, the upper-bound P of the integral sets the three-body phase, and can be related to the Efimov three-body parameter by [22]

$$P=\Lambda\frac{2}{\sqrt{3}}\exp\left[-\frac{\arctan s_0-\mathrm{Arg}[\Gamma(is_0)]+\pi\left(n-\frac{1}{2}\right)}{s_0}\right].$$

B. Nonuniversal models

1. Nonuniversal corrections

The deviations of two-body physics from universality at low energy are well known and can be encoded in the energy variation of the two-body phase shift $\delta(E)$, or, equivalently, a two-body scattering length $a(E)$. At low energy, we have the following effective-range low-energy expansion:

$$\frac{1}{a(E)}\equiv -k\cot\delta(E)=\frac{1}{a}-\frac{1}{2}r_e k^2+\cdots, \tag{5}$$

where $k=\sqrt{mE}/\hbar$. The universal limit corresponds to the first term, which is set by the zero-energy scattering length a. The next term defines the effective range r_e. It is straightforward to generalize Eq. (4) to the nonuniversal regime by replacing the zero-energy scattering length a by the energy-dependent scattering length $a(E)$ [22,30]. Likewise, the cutoff P is expected to be replaced by an energy-dependent quantity $P(E)$ [22]. With these replacements, Eq. (4) corresponds to the most general contact model with energy-dependent boundary conditions.

Although the energy dependence of $a(E)$ is generally known, that of $P(E)$ is presently unknown. It is one of the purposes of this paper to investigate this dependence by comparison with other models. As we shall see, this dependence cannot properly reproduce the full spectrum.

2. Two-body effective interaction

Another approach is to replace the real interaction by a simple effective interaction with the same low-energy spectrum. One possible choice is a Gaussian potential [31,32],

$$V(r)=-V_0 e^{-(r/r_0)^2}, \tag{6}$$

which is parametrized by V_0 and r_0 to reproduce both the scattering length and effective range. Another convenient choice is a separable interaction [20–22],

$$\hat{W}=-W_0|\phi\rangle\langle\phi|, \tag{7}$$

where the state $|\phi\rangle$ can also be chosen to be a Gaussian function $\phi(r)=e^{-(r/\sigma_0)^2}$ for simplicity. The advantage of separable potentials is that they have formal similarities with contact interactions, and lead to a simple integral equation similar to Eq. (4):

$$\left(\frac{1}{a(E)}-\sqrt{\frac{3}{4}p^2-\varepsilon}\right)F(p) + \frac{2}{\pi}\int_0^\infty dq \ln\frac{G\left[r_0^2(p^2+q^2+pq-\varepsilon)\right]}{G\left[r_0^2(p^2+q^2-pq-\varepsilon)\right]}e^{\frac{3}{8}r_0^2(q^2-p^2)}F(q)=0, \tag{8}$$

where $G(x)=\exp(\int_x^\infty \frac{e^{-t}}{t}dt)$. One can check that the integrand of (8) tends to that of (4) at low momenta, but decays at high momenta $q\gtrsim 1/r_0$, which removes the need to introduce an upper cutoff to the integral.

III. REALISTIC AND EFFECTIVE CALCULATIONS FOR $^4He_3$

A. Realistic calculations with LM2M2 potentials

To model the ^{4}He interactions realistically, we choose the LM2M2 potential [33] to describe the two-body interactions. This potential has a repulsive hard core at short distance and a van der Waals tail $-C_6/r^6$ at large distance, as shown in Fig. 1.

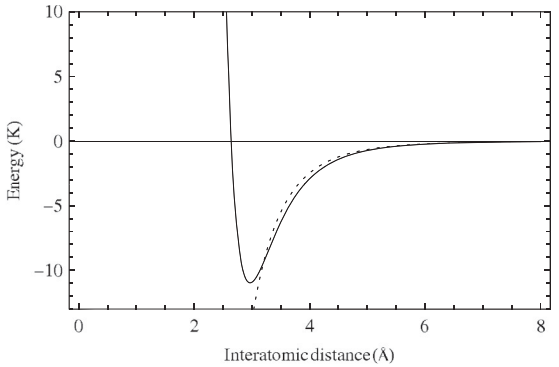

FIG. 1. LM2M2 potential [33] used for the realistic calculations. The dotted curve indicates the van der Waals asymptote $-C_6/r^6$.

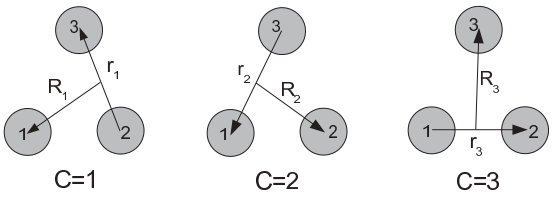

FIG. 2. Jacobi coordinates for all of the rearrangement channels ($c = 1 \sim 3$) of the ^{4}He trimer system. The wave function of the three ^{4}He atoms is to be symmetrized.

Its scattering length is 100.01 Å, which is 18.6 times the van der Waals length $l_{\rm vdW} = (mC_6/\hbar)^{1/4}$. The three-body interaction has been shown to bring only small corrections [34–36], and we neglect it in this study. Thus, in our calculation, the three-body phase, which fixes the energy of Efimov trimers, builds up only from the LM2M2 two-body interaction.

The three-body Schrödinger equation with the LM2M2 potential is solved numerically using the Gaussian expansion method (GEM). This method was proposed as a means to perform accurate calculation for three- and four-body systems [37]. In this method, a well-chosen set of Gaussian basis functions is used, forming an approximately complete set in a finite coordinate space, so that one can describe accurately both the short-range correlation and the long-range asymptotic behavior of the wave function for bound states as well as for scattering states. It was demonstrated that the GEM provides the same caliber of numerical precision as, for example, the Faddeev-Yakubovsky method for ^{3}H (^{3}He) and ^{4}He, and can be used to address various kinds of few-body problems in atomic, baryonic, and quark-level systems [37].

In order to solve the three-body ^{4}He trimer problem, we use three sets of Jacobi coordinates, illustrated in Fig. 2.

The Schrödinger equation and the total Hamiltonian are given by

$$(H - E)\Psi_{JM} = 0, \tag{9}$$

$$H = T + V(r_1) + V(r_2) + V(r_3), \tag{10}$$

where T is the kinetic-energy operator and $V(r_1)$, $V(r_2)$, and $V(r_3)$ are the interactions between two ^{4}He atoms, described by the LM2M2 potential $V(r)$.

The total three-body wave function is described as a sum of amplitudes for all rearrangement channels ($c = 1 \sim 3$) of Fig. 2:

$$\Psi_{JM} = \sum_{c=1}^{3} \sum_{n,N} \sum_{\ell,L} C^{(c)}_{nlNL} \left[\phi^{(c)}_{nl}(\mathbf{r}_c)\psi^{(c)}_{NL}(\mathbf{R}_c)\right]_{JM}. \tag{11}$$

We take the functional forms of $\phi_{nlm}(\mathbf{r})$ and $\psi_{NLM}(\mathbf{R})$ as

$$\begin{aligned} \phi_{nlm}(\mathbf{r}) &= r^l e^{-(r/r_n)^2} Y_{lm}(\widehat{\mathbf{r}}), \\ \psi_{NLM}(\mathbf{R}) &= R^L e^{-(R/R_N)^2} Y_{LM}(\widehat{\mathbf{R}}), \end{aligned} \tag{12}$$

where the Gaussian range parameters are chosen according to geometrical progressions,

$$\begin{aligned} r_n &= r_1 a^{n-1} \ (n = 1, \ldots, n_{\rm max}), \\ R_N &= R_1 A^{N-1} \ (N = 1, \ldots, N_{\rm max}). \end{aligned} \tag{13}$$

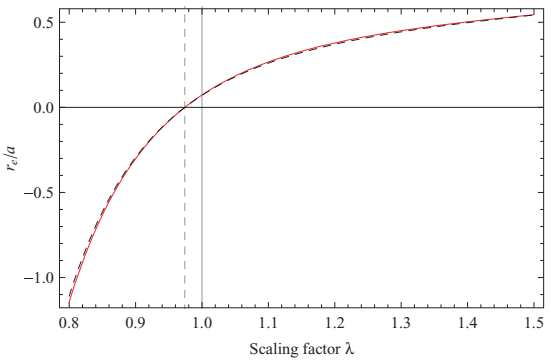

FIG. 3. (Color online) Ratio between the effective range r_e and scattering length a of the scaled LM2M2 potential as a function of the scaling factor λ. The vertical solid line indicates the physical value ($\lambda = 1$). The dashed vertical line indicates the scaling factor for which the scattering length diverges ($1/a \to 0$). The dashed curve shows the result based on the analytical formula (16) using the values of $\bar{a}$ and a as a function of λ.

The eigenenergies E in Eq. (9) and the coefficients $C^{(c)}_{nlNL}$ in Eq. (11) are determined by the Rayleigh-Ritz variational method.

Although the scattering length of ^{4}He is already large compared to the range of its two-body potential $V(r)$, we did several calculations for rescaled potentials $\lambda V(r)$ in order to cause a divergence of the scattering length, as was done in previous studies [24,25,27]. This enables us to mimic the broad Feshbach resonances used in ultracold atom experiments [38], and better appreciate the Efimov structure of the spectrum. The scattering length a diverges for $\lambda = 0.97412$, while the physical results for real ^{4}He correspond to $\lambda = 1$. As λ is varied near the divergence of a, the effective range r_e also changes but always remains positive and on the order of the scaled van der Waals length $\lambda^{1/4} l_{\rm vdW}$, and the ratio r_e/a remains a monotonic function of λ, as shown in Fig. 3. For this reason, we choose to report our results as a function of the scattering length in units of the effective range, rather than λ itself.

The LM2M2 potential supports one two-body bound state. Its energy variation with the scattering length is represented in Fig. 4. When the scattering length becomes smaller than its physical value ($\lambda \gtrsim 1.0$), this dimer energy significantly deviates from the universal limit of small binding energy and large scattering length [Eq. (14) with $a(E) \to a$]. The results for three atoms are shown in Fig. 5. Our results are in very good agreement with the most accurate calculations using the LM2M2 potential [39,40]. One can see that the first two trimers' energies qualitatively follow Efimov's universal spectrum, but as in the two-body case, there are significant deviations for small scattering lengths and deep energies. In particular, we find that neither of these two trimers connects with the dimer threshold, contrary to what is expected from the Efimov theory, although the first-excited trimer approaches very closely to that threshold (see Fig. 6).

As pointed out in Ref. [41], one way to appreciate the deviations from universality is to consider the correlations between two successive trimers. By subtracting the dimer energy from their energies, one minimizes the direct influence of the nonuniversal dimer behavior; and by considering the

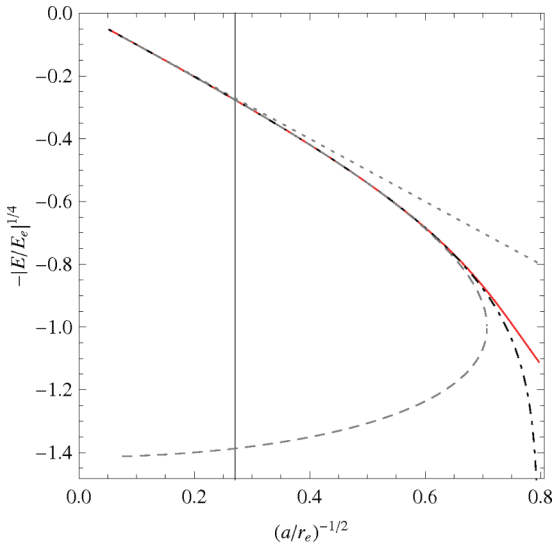

FIG. 4. (Color online) ^{4}He dimer energy E as a function of scattering length a. To clarify the figure, these quantities are normalized by $E_e = \hbar^2/mr_e^2$ and r_e, and raised to the power $1/4$ and $-1/2$, respectively. The solid red curve corresponds to the dimer of the LM2M2 potential scaled by a varying factor λ. The physical scattering length of ^{4}He ($\lambda = 1$) is indicated by the vertical gray line. The dotted line represents the universal limit of small binding energy and large scattering length [Eq. (14) with $a(E) \to a$]. The dashed curve represents the two solutions of the effective-range approximation of Eq. (14). The dot-dashed curve corresponds to the results of the separable Gaussian potential (7).

ratio between these resulting energies, one minimizes the influence of the three-body parameter. This energy ratio is represented as a function of the scattering length in Fig. 6. One can see that for an infinite scattering length, this ratio is close to the universal ratio $e^{-2\pi/s_0} \approx 1/515 \approx 0.044^2$, and then gradually deviates from the universal curve as the scattering length is decreased. It approaches zero but increases again, since the excited trimer does not quite reach the dimer threshold, while in the universal theory, the ratio vanishes when the universal trimer reaches the dimer threshold.

B. Calculation with nonuniversal corrections

We first attempt to reproduce the previous results by including nonuniversal corrections to the Efimov theory. For each value of λ, we can determine the energy dependence $a(E)$ of the scattering length of the scaled LM2M2 potential $\lambda V(r)$. The energy E_{2B} of the two-body bound state is then readily obtained from the equation

$$E_{2B} = -\frac{\hbar^2}{m[a(E_{2B})]^2}. \tag{14}$$

The low-energy expansion of $a(E)$ up to the effective-range term [right-hand side of Eq. (5)] can already reproduce the realistic two-body energy for $a \gtrsim 2.5r_e$; see Fig. 4. However, at this order of expansion, there are actually two solutions to Eq. (14), with the lowest-energy solution being unphysical. The two solutions merge and disappear at $a = 2r_e$. The presence of this extra dimer is an artifact which completely changes the three-body physics. Note that this problem does

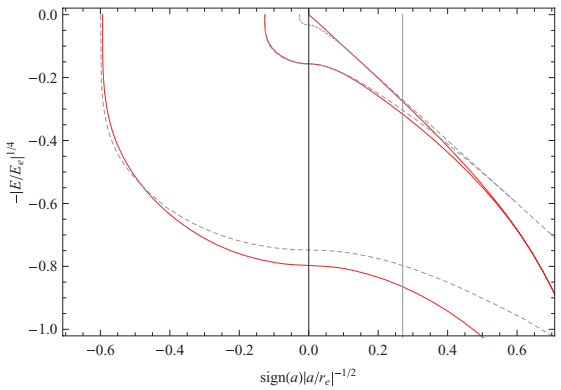

FIG. 5. (Color online) Efimov spectrum for ^{4}He: trimer energy E as a function of the scattering length a. To clarify the figure, these quantities are normalized by $E_e = \hbar^2/mr_e^2$ and r_e, and raised to the power $1/4$ and $-1/2$, respectively. The zero of the energy axis corresponds to the three-body threshold. The red solid curves are the energy curves obtained by rescaling the LM2M2 potential. The energy of both trimers and the dimer (rightmost curve) are displayed. The vertical gray line indicates the scattering length corresponding to the unscaled potential, i.e., physical ^{4}He. The dashed curves correspond to the Efimov spectrum according to the universal theory. The three-body parameter is adjusted to match the first-excited trimer state. The straight dashed line corresponds to the dimer energy in the universal limit of large scattering length.

not occur for negative effective ranges, as in the case of narrow Feshbach resonances [42]. To remedy this problem, we consider an improved analytical expression for $a(E)$ that is obtained from the separable potential given by Eq. (7) adjusted to reproduce the scattering length and effective range of the scaled LM2M2 potential. Then there is only one solution to Eq. (14) and its energy matches very well with that of the

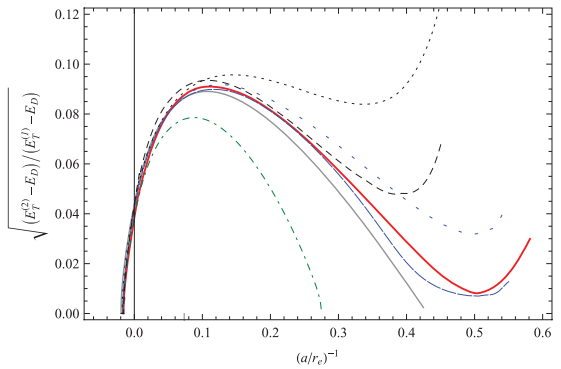

FIG. 6. (Color online) Square root of the ratio between the energies $E_T^{(1)} - E_D$ and $E_T^{(2)} - E_D$ of the first two trimers of different models as a function of the inverse scattering length (in units of r_e). Here, the trimer energy is measured from the dimer threshold E_D. The solid gray curve represents the ratio in the universal theory. The solid red curve is the result for the scaled helium LM2M2 potential. Other curves represent the results for the universal theory with two-body corrections (green dot-dashed), the local Gaussian potential model with (black dots) and without (black dashes) a three-body interaction, and the separable Gaussian potential model with (blue spaced dots) and without (blue long dashes) a three-body interaction. The vertical line indicates the point where the scattering length is infinite.

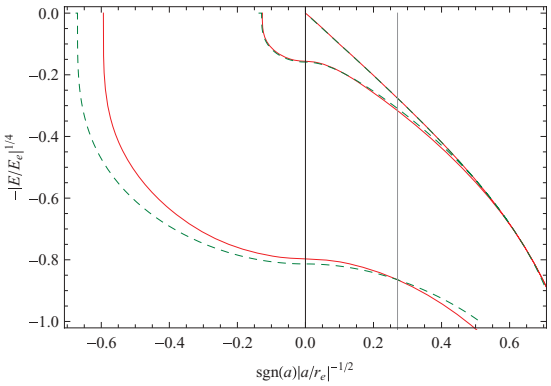

FIG. 7. (Color online) Plot similar to Fig. 5. Here again, the ^{4}He curves are indicated by solid red curves, and results taking into account two-body corrections to the universal theory are indicated by dashed curves.

LM2M2 potential; see Fig. 4. Interestingly, the agreement is even slightly better than the effective-range approximation itself.

Having set $a(E)$ to properly describe the two-body physics, we perform trimer calculations using Eq. (4) with a fixed cutoff P whose value is adjusted to reproduce the second three-body dissociation point—the point where the first-excited trimer reaches the threshold. One can see in Fig. 7 that the corrections bring some improvement, but the agreement with the LM2M2 results is only partial. It turns out that it is not possible to find an energy dependence of P that satisfactorily reproduces both the ground and first-excited trimer energies. To illustrate this, we determined the required variations of the cutoff P in order to obtain perfect agreement with the LM2M2 results for either the ground or the first-excited trimer state. The variations for both states are shown in Fig. 8 and they are inconsistent. To remove the inconsistency, we can assume more generally that P depends on both the energy and the scattering length, but no clear pattern arises from such considerations. It should also be noted that the required variation of P is dependent on the choice of the high-energy behavior of $a(E)$; in other words, it is model dependent. Thus, while it can be a practical way to characterize nonuniversal observations, as done in Refs. [15, 16,22], it does not seem to be very meaningful.

C. Calculations with a separable potential

We then attempt to reproduce the ^{4}He results with a simple two-body potential V having the same low-energy properties as the LM2M2 potential. For both the Gaussian potential (6) and separable potential (7), we proceed as follows.

For each λ, we adjust the parameters of the potential so that the scattering length and effective range coincide with those of the scaled LM2M2 potential. As mentioned before, the binding energy of the two-body bound state then matches very well with that of the LM2M2 bound state over a wide range of energies; see Fig. 4.

We then calculate the three-body bound states with the adjusted potential. Remarkably, we already find relatively good agreement with the LM2M2 three-body states; see Figs. 9 and 10. The values differ essentially by an energy shift, which is not unexpected since the short-range three-body phase may not be properly set by these simple two-body interactions.

As a practical way to set the proper three-body phase, we finally add to the effective models a three-body interaction, and adjust its strength in order to reproduce the second three-body dissociation point. We again use a simple local or separable Gaussian form for the three-body interaction, specifically Eqs. (6) and (7), where r is replaced by the hyper-radius R defined in Eq. (1). We use the parameters $V_0^{(3B)} = 0.43\frac{\hbar^2}{m}r_0^{-2}$ and $r_0^{(3B)} = 0.5r_0$ for the local potential, and $W_0^{(3B)} = 0.165\frac{\hbar^2}{m}\sigma_0^{-8}$ and $\sigma_0^{(3B)} = 1.0\sigma_0$ for the separable potential.

We then find very good overall agreement for both trimers with the LM2M2 calculations, as shown in Figs. 9 and 10. The agreement with the excited trimer is good, except when its energy approaches the two-body threshold, as seen in Fig. 6. This disagreement corresponds to small energy differences when compared to the total binding energy of the dimer or trimer measured from the three-body threshold.

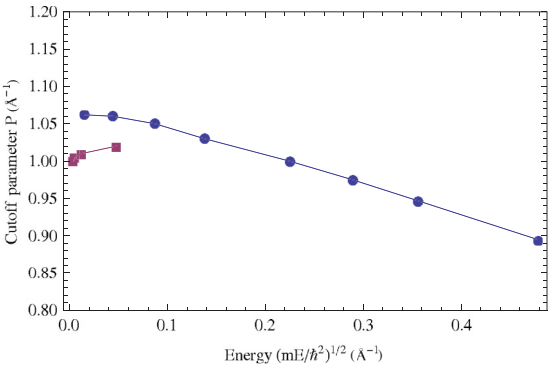

FIG. 8. (Color online) Three-body cutoff parameter P adjusted to get agreement with the LM2M2 results as a function of energy for the ground-state trimer (dots) and the first excited-state trimer (squares). One can see that their variations are inconsistent.

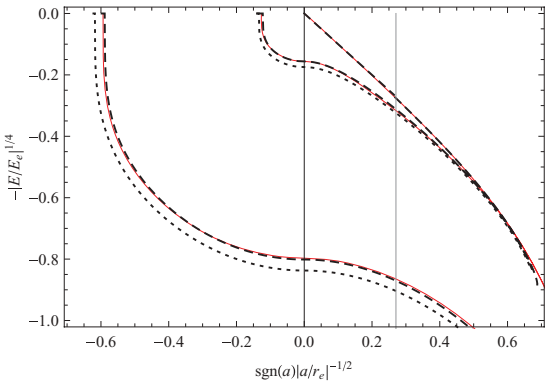

FIG. 9. (Color online) Plot similar to Fig. 5 for the calculations with the Gaussian potential given by Eq. (6). The dotted curves correspond to two-body interactions only, while the dashed curves correspond to calculations with an additional three-body interaction.

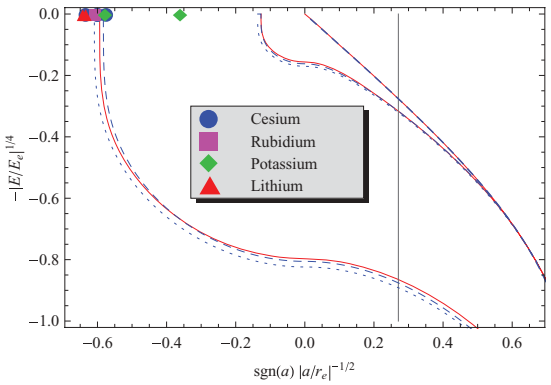

FIG. 10. (Color online) Plot similar to Fig. 5 for the calculations with the separable Gaussian potential given by Eq. (7). The dotted curves correspond to two-body interactions only, while the dashed curves correspond to calculation with an additional three-body interaction. The symbols show the measured dissociation point of the ground-state trimer for different species. One data point from the experiments with potassium lies outside the group of data points, and it is not clear whether this is a special feature of that species breaking the observed tendency or due to a misinterpretation of the data.

D. Role of the effective range

1. Trimer dissociation at the three-body threshold

The previous results clearly indicate that the nonuniversal variations of the trimer energies can be reproduced to a great extent from the knowledge of the effective range. The role of the effective range was pointed out before in previous studies [18,19,30,32]. In particular, Ref. [32] also looked at deviations from universality with finite-range potentials. This study considered the scattering length a_{diss} for which the trimer dissociates into three atoms. The relative variation of this quantity with respect to its value a'_{diss} in the universal spectrum was found to be

$$\frac{a_{\mathrm{diss}} - a'_{\mathrm{diss}}}{a'_{\mathrm{diss}}} = C\left(\frac{r_e}{a}\right)_{\mathrm{diss}}, \tag{15}$$

with $C = 1.3 \pm 0.4$. However, we could not completely confirm this formula. While we found the value $C \approx 0.99$ with the Gaussian potential, which is consistent with the results presented in Ref. [32] for the same Gaussian potential, the present calculation with the LM2M2 potential gives $C \approx 0.58$. The value therefore seems to be somewhat dependent on the type of potential.

It is interesting to note that the value of the dissociation point a_{diss} itself, rather than its nonuniversal variation, was found experimentally to be in a narrow range. Experimentalists have measured the ground-state trimer dissociation point near several Feshbach resonances causing a divergence of the scattering lengths [17], for different species [2,3,6,9,10,14,17], and found that it almost always occurs around $a_{\mathrm{diss}} \approx -9.9\bar{a}$, where $\bar{a} = 2\pi/\Gamma(1/4)^2 l_{\mathrm{vdW}}$ is the average scattering length of van der Waals potentials [38]. Since there is an approximate relation between $\bar{a}$ and the effective range r_e [43,44],

$$\frac{r_e}{a} = \frac{2}{3}\frac{\Gamma(1/4)^4}{(2\pi)^2}\frac{\bar{a}}{a}\left[\left(\frac{\bar{a}}{a}\right)^2 + \left(\frac{\bar{a}}{a} - 1\right)^2\right], \tag{16}$$

this corresponds to $a_{\mathrm{diss}}/r_e \approx -2.76$. Experimental measurements of a_{diss}/r_e for different species are represented in Fig. 10. It is quite remarkable that the scaled helium potential also gives a dissociation point $a_{\mathrm{diss}}/r_e \approx -2.82$ (or, equivalently, $a_{\mathrm{diss}}/\bar{a} = -10.26$) which lies in the same narrow range. Furthermore, the model potentials considered in this paper (Gaussian and separable potential), without any three-body interaction, also give a consistent value $a_{\mathrm{diss}}/r_e \approx -2.70$ of the dissociation point. This shows that the use of these model potentials to interpret experiments leads to a good estimate of the dissociation point, as noted before [21,22]. Why it does so is, however, a puzzling question, since we know from calculations with other or deeper potentials that the dissociation point can change significantly [23]. This suggests that under some condition yet to be understood, the effective range may not only determine the nonuniversal variations, but also the three-body parameter, thereby determining the full low-energy three-body spectrum [45].

2. Trimer dissociation at the dimer threshold

In the universal theory, the trimers dissociate at the dimer threshold at some positive value of the scattering length. As we have already pointed out, in our calculations, because of the finite-range effects, the excited trimer does not dissociate but rather comes very close to the dimer threshold before eventually going away from it. This can be seen from the local minimum in Fig. 6. This nonuniversal feature is qualitatively reproduced by the local and separable Gaussian potential models, but the height and location of the minimum are different for different models.

This suggests that in general the trimer energy near the dimer threshold depends on details of the potential other than the effective range. Therefore, such a model dependence could explain the fact that models based on the effective range could not reproduce the nonuniversal deviations of the trimer energy near the dimer threshold which were experimentally observed in [15,16]. The situation studied here, however, is a shape resonance obtained by scaling the interaction potential, which is not the same as the Feshbach resonances used in the experiments. Besides the possibility of underestimated uncertainties in the models or the experiments, other effects such as multichannel couplings and nontrivial effects of three-body forces could also play a role.

IV. CONCLUSION

In this work, we have studied the Efimov physics of three ^{4}He atoms as a simple but realistic example to understand the nonuniversal variations of the trimer energy with respect to the scattering length. We found that nonuniversal two-body corrections to the universal theory alone are not sufficient to fully reproduce these variations, and a variable three-body parameter is needed. However, the variations of this three-body parameter do not seem to follow any simple rule, and are model dependent. On the other hand, *ad hoc* but simple two-body potentials, such as separable Gaussian potentials adjusted to have the same scattering length and effective range,

reproduce remarkably well the nonuniversal variations of the trimer energy, and can constitute relatively accurate substitutes for single-channel realistic interactions provided that a small and localized three-body force is introduced to properly shift the energy. These results suggest that, in general, beyond the usual Efimov universal scenario occurring for higher-excited trimers, the whole spectrum follows a more specific class of universality determined only by the scattering length, the effective range, and the strength of a three-body localized force setting the three-body parameter, i.e., the position of highly-excited trimers.

ACKNOWLEDGMENTS

We thank F. Ferlaino, R. Grimm, P.S. Julienne, J. D'Incao, C. H. Greene, and E. Braaten for helpful discussions. Some of the numerical calculations were performed on the HITACHI SR11000 at KEK.

[1] V. N. Efimov, Sov. J. Nucl. Phys. **12**, 589 (1971); Nucl. Phys. A **210**, 157 (1973).
[2] F. Ferlaino and R. Grimm, Physics **3**, 9 (2010).
[3] T. Kraemer *et al*., Nature (London) **440**, 315 (2006).
[4] T. B. Ottenstein, T. Lompe, M. Kohnen, A. N. Wenz, and S. Jochim, Phys. Rev. Lett. **101**, 203202 (2008).
[5] J. R. Williams, E. L. Hazlett, J. H. Huckans, R. W. Stites, Y. Zhang, and K. M. O'Hara, Phys. Rev. Lett. **103**, 130404 (2009).
[6] M. Zaccanti *et al*., Nature Phys. **5**, 586 (2009).
[7] G. Barontini, C. Weber, F. Rabatti, J. Catani, G. Thalhammer, M. Inguscio, and F. Minardi, Phys. Rev. Lett. **103**, 043201 (2009).
[8] A. N. Wenz, T. Lompe, T. B. Ottenstein, F. Serwane, G. Zurn, and S. Jochim, Phys. Rev. A **80**, 040702 (2009).
[9] S. E. Pollack, D. Dries, and R. G. Hulet, Science **326**, 1683 (2009).
[10] N. Gross, Z. Shotan, S. Kokkelmans, and L. Khaykovich, Phys. Rev. Lett. **103**, 163202 (2009).
[11] J. H. Huckans, J. R. Williams, E. L. Hazlett, R. W. Stites, and K. M. O'Hara, Phys. Rev. Lett. **102**, 165302 (2009).
[12] T. Lompe, T. B. Ottenstein, F. Serwane, K. Viering, A. N. Wenz, G. Zurn, and S. Jochim, Phys. Rev. Lett. **105**, 103201 (2010).
[13] T. Lompe *et al*., Science **330**, 940 (2010).
[14] N. Gross, Z. Shotan, S. Kokkelmans, and L. Khaykovich, Phys. Rev. Lett. **105**, 103203 (2010).
[15] S. Nakajima, M. Horikoshi, T. Mukaiyama, P. Naidon, and M. Ueda, Phys. Rev. Lett. **105**, 023201 (2010).
[16] S. Nakajima, M. Horikoshi, T. Mukaiyama, P. Naidon, and M. Ueda, Phys. Rev. Lett. **106**, 143201 (2011).
[17] M. Berninger, A. Zenesini, B. Huang, W. Harm, H. C. Nagerl, F. Ferlaino, R. Grimm, P. S. Julienne, and J. M. Hutson, Phys. Rev. Lett. **107**, 120401 (2011).
[18] Lucas Platter, Chen Ji, and Daniel R. Phillips, Phys. Rev. A **79**, 022702 (2009).
[19] C. Ji, L. Platter, and D. R. Phillips, Europhys. Lett. **92**, 13003 (2010).
[20] M. D. Lee, T. Köhler, and P. S. Julienne, Phys. Rev. A **76**, 012720 (2007).
[21] M. Jona-Lasinio and L. Pricoupenko, Phys. Rev. Lett. **104**, 023201 (2010).
[22] P. Naidon and M. Ueda, arXiv:1008.2260; C. R. Phys. **12**, 13 (2010).
[23] J. P. D'Incao, C. H. Greene, and B. D. Esry, J. Phys. B **42**, 044016 (2009).
[24] T. Cornelius and W. Glöckle, J. Chem. Phys. **85**, 3906 (1986).
[25] B. D. Esry, C. D. Lin, and Chris H. Greene, Phys. Rev. A **54**, 394 (1996).
[26] E. Nielsen, D. V. Fedorov, and A. S. Jensen, J. Phys. B **31**, 4085 (1998).
[27] T. González-Lezana, J. Rubayo-Soneira, S. Miret-Artes, F. A. Gianturco, G. Delgado-Barrio, and P. Villarreal, Phys. Rev. Lett. **82**, 1648 (1999).
[28] Eric Braaten and H.-W. Hammer, Phys. Rev. A **67**, 042706 (2003).
[29] G. V. Skorniakov and K. A. Ter-Martirosian, Sov. Phys. JETP **4**, 648 (1957).
[30] V. Efimov, Phys. Rev. C **44**, 2303 (1991).
[31] A. Kievsky, E. Garrido, C. Romero-Redondo, and P. Barletta, Few-Body Syst. **51**, 259 (2011).
[32] M. Thøgersen, D. V. Fedorov, and A. S. Jensen, Phys. Rev. A **78**, 020501R (2008).
[33] R. A. Aziz and M. J. Slaman, J. Chem. Phys. **94**, 8047 (1991).
[34] C. A. Parish and C. E. Dykstra, J. Chem. Phys. **101**, 7618 (1994).
[35] I. Røeggen and J. Almlöf, J. Chem. Phys. **102**, 7095 (1995).
[36] W. Cencek, M. Jeziorska, O. Akin-Ojo, and K. Szalewicz, J. Phys. Chem. A **111**, 11311 (2007).
[37] E. Hiyama, Y. Kino, and M. Kamimura, Prog. Part. Nucl. Phys. **51**, 223 (2003).
[38] C. Chin, R. Grimm, P. Julienne, and E. Tiesinga, Rev. Mod. Phys. **82**, 1225 (2010).
[39] D. Blume and C. H. Greene, J. Chem. Phys. **112**, 8053 (2000).
[40] R. Lazauskas and J. Carbonell, Phys. Rev. A **73**, 062717 (2006).
[41] T. Frederico, L. Tomio, A. Delfino, and A. E. A. Amorim, Phys. Rev. A **60**, R9 (1999).
[42] D. S. Petrov, Phys. Rev. Lett. **93**, 143201 (2004).
[43] B. Gao, Phys. Rev. A **58**, 4222 (1998).
[44] V. V. Flambaum, G. F. Gribakin, and C. Harabati, Phys. Rev. A **59**, 1998 (1999).
[45] Recently, a preprint presenting calculations with various potentials confirmed that such a situation happens when the potential is deep or repulsive enough; see arXiv:1201.1176. The potentials we use are shallow, although the LM2M2 potential has a strong repulsive core. It is unclear whether our results can be related to the effect found in that study.